https://doi.org/10.5194/acp-2020-46
Preprint. Discussion started: 31 January 2020

Atmospheric Chemistry and Physics Discussions

The impact of weather pattern and related transport processes on aviation's contribution to ozone and methane concentrations from NO_x emissions

Simon Rosanka[1,a], Christine Frömming[2], and Volker Grewe[1,2]

[1]Delft University of Technology, Faculty of Aerospace Engineering, Section Aircraft Noise Climate Effects, Delft, The Netherlands
[2]Deutsches Zentrum für Luft- und Raumfahrt, Institute of Atmospheric Physics, Oberpfaffenhofen, Germany
[a]now at: Forschungszentrum Jülich GmbH, Institute of Energy and Climate Research, IEK-8: Troposphere, Jülich, Germany

Correspondence: Volker Grewe (volker.grewe@dlr.de)

Abstract. Aviation attributed climate impact depends on a combination of composition changes in trace gases due to emissions of carbon dioxide (CO_2) and non-CO_2 species. Nitrogen oxide ($NO_x = NO + NO_2$) emissions lead to an increase in ozone (O_3) and a depletion of methane (CH_4), whereas water vapour (H_2O) can additionally lead to the formation of persistent contrails. In comparison to CO_2, non-CO_2 contributions to the atmospheric composition are short lived and are thus characterised by a high spatial and temporal variability. In this study, we investigate the influence of weather pattern and their related transport processes on composition changes caused by aviation attributed NO_x emissions, by using the atmospheric chemistry model EMAC (ECHAM/MESSy). Representative weather situations are simulated in which unit NO_x emissions are initialised in specific air parcels at typical flight altitudes over the North Atlantic flight sector. By explicitly calculating composition changes induced by these emissions, interactions between trace gas composition changes and weather conditions along the trajectory of each air parcel are investigated.

The resulting climate impact from NO_x via changes of O_3 mainly depends on the magnitude of the maximum induced composition change. In general, the earlier the maximum O_3 change occurs the larger the total O_3 change and therefore the resulting climate impact. In this study we show that subsidence in high pressure systems leads to an earlier O_3 maximum and that the maximum O_3 change is limited by atmospheric NO_x and HO_2 during summer and winter, respectively. The resulting climate impact due to composition changes of CH_4 depends only on the magnitude of the induced depletion of CH_4, where a larger depletion of CH_4 leads to a larger cooling effect. We show that a large CH_4 depletion is only possible if a strong formation of O_3 occurs and if large atmospheric H_2O concentrations are present. Only air parcels which are transported into tropical areas, due to high pressure systems, experience high concentrations of H_2O and thus a large CH_4 depletion.

Re-routing flight trajectories based on the experimental setup used in this study is currently too computationally expensive. This work demonstrates that transport processes are of most interest when identifying the climate impact from aviation NO_x emissions. The insights gained in this study suggest an approach to re-route flights in the future, by performing less computationally expensive purely dynamic simulations.

https://doi.org/10.5194/acp-2020-46
Preprint. Discussion started: 31 January 2020

Atmospheric Chemistry and Physics Discussions

1 Introduction

The importance of anthropogenic climate change has been well established since years (Shine et al., 1990) and it is well known that air traffic contributes substantially to the total anthropogenic climate change (Lee et al., 2009; Brasseur et al., 2016; Grewe et al., 2017a). A major fraction of its contribution comes from non-CO_2 emissions which lead to changes in greenhouse gas concentrations as well as contrail and contrail-cirrus formation in the atmosphere (Kärcher, 2018). The climate impact of CO_2 is mainly characterised by the emissions strength, due to its long lifetime. However, non-CO_2 effects are known to be characterised by a high spatial and temporal variability. This implies that the total contribution to concentrations of non-CO_2 emissions is not only influenced by the emissions strength but also by the time and location of the emission itself.

The emission of nitrogen oxides (NO_x = NO + NO_2) leads to changes in ozone and methane concentrations. Additional concentration changes in ozone are introduced by changes to the precursor methane, known as primary mode ozone (PMO) (Wild et al., 2001). Earlier studies already identified that the climate impact resulting from aviation attributed NO_x emissions varies strongly within the atmosphere. Köhler et al. (2013) showed that the climate impact is larger for emissions occurring in lower than in higher latitudes. A larger climate impact also occurs in regions with low aviation activity (such as in low altitudes) for the same amount of NO_x. Both can be explained by higher incoming solar radiation and lower background NO_x concentrations in those regions compared to higher latitudes. A similar impact was identified by Stevenson and Derwent (2009). The general lower background NO_x concentration in the Southern Hemisphere (SH) compared to the Northern Hemisphere (NH) also explains the inter-hemispheric discrepancy of the resulting climate impact from NO_x emissions. In the SH the climate impact from the same amount of NO_x is generally larger. Köhler et al. (2008) identified that the emission altitude strongly influences the resulting climate impact and is generally larger for emissions at high altitudes. Frömming et al. (2012) demonstrated that the overall climate impact can be reduced by adopting flight altitudes, suggesting a possible mitigation strategy. The season in which the emission occurs influences the resulting climate impact in addition to the emission location. Gilmore et al. (2013) identified that during summer the climate impact is up to 1.5 times higher and only half in winter, when compared to the annual mean. Grewe et al. (2017a) and Frömming et al. (2020) demonstrated that the total change in ozone is larger if the NO_x emission occurred within a high pressure ridge compared to emissions occurring west of this blocking condition. This shows that the impact of aviation NO_x emissions depends on weather situation at the time of emission and along the trajectory. Further investigations are necessary to improve the understanding of those emissions to provide possible mitigation strategies in the future.

In the present study, we investigate the impact of weather situations on changes in ozone and methane concentrations induced by NO_x emissions in the upper troposphere, emitted over the North Atlantic flight sector. Here, special focus is on how weather conditions influence the length of the time period in which O_3 is mainly produced, the total O_3 gained as well as the total CH_4 depleted. Our findings are additionally analysed with respect to inter-seasonal variability. This is achieved by using the results of simulations performed in the European project REACT4C (Reducing Emissions from Aviation by Changing Trajectories for the benefit of Climate, https://www.react4c.eu/ (Matthes, 2011)). REACT4C was intended to elaborate the feasibility of adopting flight altitudes and routes to minimise the climate impact of aviation and estimated the global effect of such an air

https://doi.org/10.5194/acp-2020-46
Preprint. Discussion started: 31 January 2020

Atmospheric Chemistry and Physics Discussions

traffic management measure in the North Atlantic flight sector (Grewe et al., 2014, 2017b). Within this analysis, interactions between weather conditions and trace gas concentration changes along the trajectory of each air parcel in which the NO_x emission occurs are investigated. The modelling approach of REACT4C as well as the methodology used in this study is elaborated in Section 2. Characteristics of changes in ozone and methane concentrations induced by NO_x emissions will be analysed in Section 3. Afterwards all findings of this study will be presented (Section 4). In Section 5 uncertainties and findings in this study will be discussed. Possible implementation strategies are presented in the conclusion (Section 6).

2 Methodology

Our analysis of the general concept of REACT4C as well as the modelling approach used will be elaborated first to understand how the impacts of NO_x emissions on O_3 and CH_4 were simulated. The idea of the project is presented by Matthes (2011) and Matthes et al. (2012). A complete description of the modelling approach used is given by Grewe et al. (2014). Afterwards, a detailed description of the steps taken within our analysis is presented.

2.1 REACT4C

REACT4C investigated the feasibility of adopting flight routes and flight altitudes to minimise the climate impact of aviation and estimate the global effect of such air traffic management (ATM) measures (Grewe et al., 2014). In this particular study, this mitigation option was tested over the North Atlantic region. The general steps in this modelling approach were as follows: (1) select representative weather pattern, (2) define time-regions, (3) model atmospheric contribution for additional emissions in these time-regions, (4) calculate the adjusted radiative forcing (RF), (5) calculate the climate change function (CCF) for each emission species and induced cloudiness, (6) optimize aircraft trajectories, based on the CCF results, by using an air traffic simulation system (System for traffic Assignment and Analysis at a Macroscopic level, SAAM) which is coupled to an emission tool (Advanced Emission Model, AEM), and (7) calculate the resulting operation costs and the resulting climate impact reduction. For the present study, only step one to five are important and will be further elaborated.

Irvine et al. (2013) identified, that by simulating frequently occurring weather situations within a season, the global seasonal impact can be estimated. They analysed meteorological reanalysis data for 21 years of summer and winter. This reanalysis leads to three distinct summer (SP1-3) and five winter patterns (WP1-5). The different weather patterns mainly vary in their location, orientation and strength of the jet stream and the phase of the North Atlantic Oscillation and the Arctic Oscillation, two distinct teleconnection pattern. A graphical representation of each defined weather pattern is given by Irvine et al. (2013, Figure 7 and Figure 8 for winter and summer, respectively) and the actual weather situation simulated in REACT4C are presented in Frömming et al. (2020). Due to the lower variability of the jet stream in summer, only three distinct weather situations were determined. Analogously, REACT4C simulated eight distinct model days, each representing one of these weather patterns. The summer pattern occur 19 (SP1), 55 (SP2) and 18 (SP3) and the winter pattern 17 (WP1 & WP2), 15 (WP3 & WP4) and 26 (WP5) times per season in the reanalysis data (Irvine et al., 2013).

https://doi.org/10.5194/acp-2020-46
Preprint. Discussion started: 31 January 2020


Atmospheric Chemistry and Physics Discussions

To calculate the climate change functions, a time-region grid was defined in the North Atlantic region for seven latitudes (between 30°N to 80°N) and six longitudes (between 80°W to 0°W) over 4 different pressure levels (200, 250, 300 and 400 hPa) to account for different flight levels. At each time-region grid point unit emissions of CO_2, NO_x and H_2O are initialised on 50 trajectories at 6, 12 and 18 UTC. However, in the present study, only 12 UTC is considered. The 50 trajectories are randomly located in the respective model grid box in which the specific time-region grid point is located. At each time-region grid point 5×10^5 kg of NO (equals 2.33×10^5 kg(N)) are emitted, which is then equally distributed onto the trajectories (Grewe et al., 2014).

2.2 Base model description

The ECHAM/MESSy Atmospheric Chemistry (EMAC) model is a numerical chemistry and climate simulation system that includes sub-models describing tropospheric and middle atmosphere processes and their interaction with oceans, land and human influences (Jöckel et al., 2010). It uses the second version of the Modular Earth Submodel System (MESSy2) to link multi-institutional computer codes. The core atmospheric model is the 5th generation European Centre Hamburg general circulation model (ECHAM5, Roeckner et al. (2003)). For the present study we applied EMAC (ECHAM5 version 5.3.02, MESSy version 2.52.0) in the T42L41-resolution, i.e. with a spherical truncation of T42 (corresponding to a quadratic Gaussian grid of approximately 2.8 by 2.8 degrees in latitude and longitude) with 41 vertical hybrid pressure levels up to 5 hPa.

The applied model setup comprised multiple MESSy submodules important for the performed simulations. Each of the tracers (i.e. NO_x and H_2O) is emitted in an air parcel by the submodel Tracer Release EXperiments from Point sources (TREXP). The air parcel is then advected by the submodel Atmospheric Tracer Transport In a LAgrangian model (ATTILA) (Reithmeier and Sausen, 2002). For each trajectory the contribution of the emission (i.e. NO_x and H_2O) to the atmospheric concentration of CH_4, O_3, HNO_3, H_2O and OH is calculated over a time period of 90 days by using the submodel AIRTRAC (version 1.0, Frömming et al. (2013); see Supplement of Grewe et al. (2014)). The tagging approach used by AIRTRAC was first described by Grewe et al. (2010). In this approach each important chemical reaction is doubled. The first reaction applies to the whole atmosphere (from here onwards referred to as background) and the second one only to the additionally emitted tracer (from here onwards referred to as foreground). The submodel MECCA (Module Efficiently Calculating the Chemistry of the Atmosphere) is used to model the background chemical processes in the troposphere and stratosphere. The chemical mechanism used by MECCA can be grouped into sulfur, non-CH_4 hydrocarbon, basic O_3, CH_4, HO_x and NO_x and halogen chemistry (Sander et al., 2005). AIRTRAC on the other hand calculates the resulting changes due to the additional emitted NO_x in the foreground. AIRTRAC assumes that each concentration change of O_3 due to aviation is attributed to the emitted NO_x, which is consistent with Brasseur et al. (1998). Concentration changes due to additionally emitted NO_x are calculated based on the concentration of all chemical species involved in the general chemical system and the concentrations due to the extra emitted NO_x. The actual concentration change is then calculated based on the background reaction rate and the fraction of foreground and background concentrations of all reactants (Grewe et al., 2010). In detail, the foreground loss of O_3 ($L^f_{O_3}$)

https://doi.org/10.5194/acp-2020-46
Preprint. Discussion started: 31 January 2020

Atmospheric Chemistry and Physics Discussions

via Reaction R1 is based on the foreground and background concentrations of NO_2 and O_3 (NO_2^f, O_3^f and NO_2^b, O_3^b for foreground and background, respectively) and the background loss of O_3 ($L_{O_3}^b$), as given in Equation 1.

$$NO_2 + O_3 \rightarrow NO + 2O_2 \tag{R1}$$

$$L_{O_3}^f = L_{O_3}^b \times \frac{1}{2}\left(\frac{NO_2^f}{NO_2^b} + \frac{O_3^f}{O_3^b}\right) \tag{1}$$

In total AIRTRAC calculates the mass development of NO_x, O_3, HNO_3, OH, HO_2 and H_2O by tracking 14 reactions and reaction groups. One group for the production and one for the destruction of O_3 as well as one for the formation of HNO_3 is tracked. Three and five reactions are tracked for the OH production and destruction, respectively. In addition three reaction groups for the production and destruction of HO_2 are tracked. Further loss processes like wash-out and deposition are taken into account (Grewe et al., 2014). The results of this mechanism agrees well with earlier studies with respect to the regionally different chemical regimes and the overall effect of aviation emissions (Grewe et al., 2017c, Section 4.3, therein). The tagging mechanism also enables the quantification of methane losses due to the two major reaction pathways, the change in HO_x partitioning towards OH due to a NO_x emission and the production of OH due to an enhanced ozone concentration (Grewe et al., 2017c, Figure 8).

2.3 Analysis performed in this study

Within this study we used the simulation output created by the REACT4C project. As some output variables were not available for all emission locations and weather patterns, not all time regions and weather pattern could be included in the present study. Emissions occurred in a time region grid of 7 latitudes, 6 longitudes and 4 pressure levels at 12 UTC. From originally 1344, 1115 emission locations are analysed. At each emission location all 50 air parcels are taken into account, resulting in 55750 trajectories being analysed. An output resolution of six hours was used by REACT4C over 90 days.

The variables taken into account in this analysis can be categorised into three different groups: (1) background and foreground chemical concentrations, (2) background and foreground chemical reaction rates and (3) general weather information. All foreground variables are present on the tracer grid (trajectory id and time), whereas background data are stored on the original EMAC grid. To simplify our analysis, background data were re-gridded onto the tracer grid. Here it was assumed that all background data within a grid box are valid for each air parcel within this specific EMAC grid box.

Due to the general complexity of the atmospheric chemistry, many variables can potentially influence changes in O_3 and CH_4 concentrations induced by NO_x emissions. Therefore, correlation matrices were used to identify interacting parameters. For these matrices the three most common statistical measures to identify correlations were used (Pearson, Kendall, and Spearman's rank correlation coefficient). Statistical significance is ensured by using t-, one-way analysis of variance (ANOVA) and Tukey's honest significant difference (HSD) tests.

https://doi.org/10.5194/acp-2020-46
Preprint. Discussion started: 31 January 2020

Atmospheric Chemistry and Physics Discussions

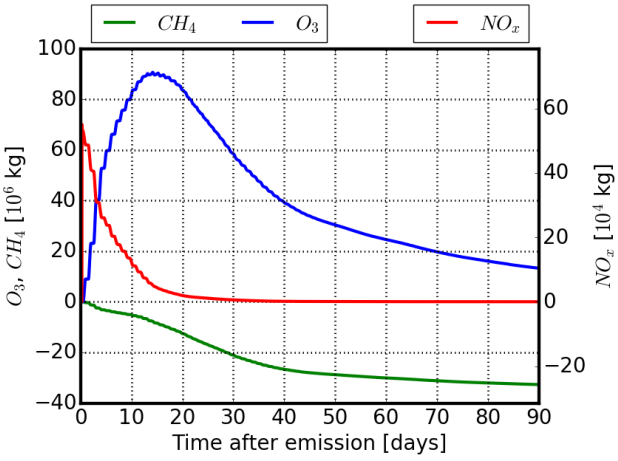

Figure 1. Changes in O_3 and CH_4 concentrations introduced by an emitted unit emission of NO_x (emission strength: 5×10^5 kg of NO).

3 Characteristics of the temporal development of O_3 and CH_4 due to NO_x

In the upper troposphere O_3 is mainly produced by a catalytic reaction including NO_x. Emitted NO reacts with HO_2 forming NO_2. Via photodissociation, NO_2 forms $O(^3P)$ which leads to the production of O_3 (Reaction R2 - R4).

$$HO_2 + NO \rightarrow OH + NO_2 \quad \text{(R2)}$$

$$NO_2 + h\nu(\lambda \leq 410nm) \rightarrow NO + O(^3P) \quad \text{(R3)}$$

$$O(^3P) + O_2 + M \rightarrow O_3 + M \quad \text{(R4)}$$

The additionally formed OH leads to an oxidation of CH_4:

$$CH_4 + OH \rightarrow CH_3 + H_2O \quad \text{(R5)}$$

Figure 1 shows the "typical" temporal development of O_3 and CH_4 due to an aviation attributed NO_x emission. NO_x is reduced almost exponentially and washed out after about a month. While the emitted NO_x decreases, the O_3 concentration increases due to the described production processes (Reaction R2 -R4). When the NO_x mixing ratio is below a certain level, no further O_3 is produced and loss terms dominate the O_3 chemistry. The additionally formed O_3 continuously decreases and reaches zero after about three months. At the same time the additional O_3 and NO_x form OH leading to a depletion of CH_4

https://doi.org/10.5194/acp-2020-46
Preprint. Discussion started: 31 January 2020

Atmospheric Chemistry and Physics Discussions

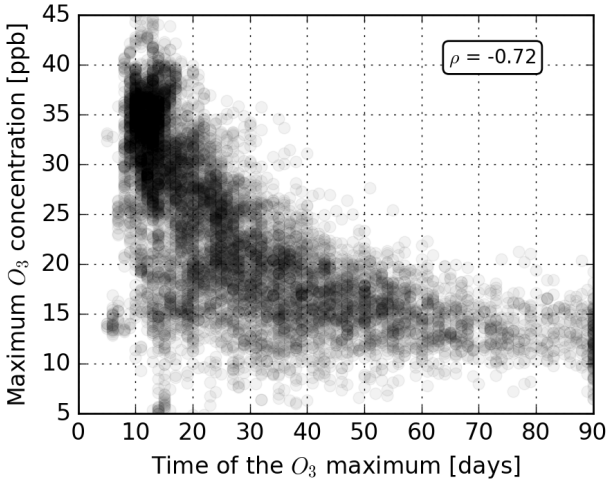

Figure 2. Maximum O_3 concentration in relation to the time when the O_3 maximum is reached. Data are taken from the first winter pattern. The Spearman rank correlation coefficient ρ is provided as a statistical measure.

(Reaction R5). After all NO_x and O_3 is lost, the negative CH_4 anomaly starts to decay and will later reach its original values (not seen in Figure 1). There is a large variability in this NO_x-O_3-CH_4 relation, which is presented in Figure 9 of Grewe et al. (2014). In the following we analyse, which parameters lead to this large variability.

Figure 2 shows the maximum O_3 concentration in relation to the time after emission when the maximum occurs. A high concentration change is only possible if the O_3 maximum occurs early. About 47.5 % and 72 % of all air parcels reach their O_3 maximum within the first 21 days during winter and summer, respectively. Only a small number of air parcels reach their maximum at the end of simulation (winter: 2.5%, summer: 1%). All air parcels with a late maximum are emitted at higher altitudes (200 or 250 hPa). It is known that the concentration change of O_3 is not the only factor that influences the resulting radiative forcing. Lacis et al. (1990) demonstrated that also the altitude at which the concentration change occurs plays a significant role on the radiative impact. The climate impact increases from the surface towards the tropopause, then decreases again resulting in a cooling effect in the lower stratosphere above 30 km. Within the REACT4C experiment a higher O_3 concentration change generally leads to a larger RF (Spearman rank coefficient of 0.74). Even though the RF is only an approximation of the CCF, the time and magnitude of the O_3 maximum influence its potential climate impact. Both characteristics are thus analysed within this study. In contrast, the RF due to a depletion of CH_4 is considered to be proportional to the total CH_4 loss. This is due to the long tropospheric lifetime of CH_4. Therefore, focus will be on the total CH_4 depletion, only.

https://doi.org/10.5194/acp-2020-46
Preprint. Discussion started: 31 January 2020

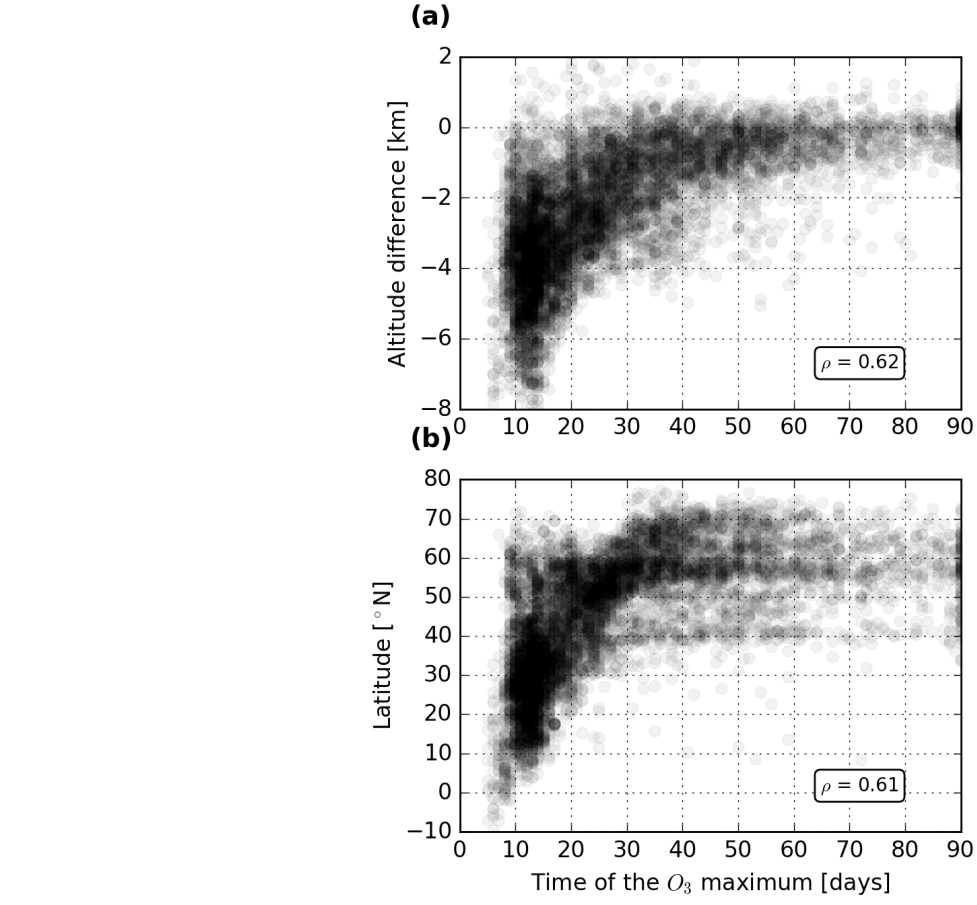

Figure 3. (a) Mean altitude of air parcels at the time of the O_3 maximum relative to the emission altitude. (b) Mean latitude of air parcels at the time of the O_3 maximum. The analysis is based on the first seven day after emission. Data are taken from WP1. The Spearman rank correlation coefficient ρ is provided as a statistical measure.

4 Results

Within this section, the results of this study are described. The influence of transport processes on the time of the O_3 maximum is analysed in Section 4.1. The mechanisms controlling total O_3 change are investigated in Section 4.2 and 4.3 for summer and winter, respectively. The influence of tropospheric water vapour on total CH_4 depletion is discussed in Section 4.4. These findings are presented for representative weather patterns. An inter-seasonal variability analysis is performed in Section 4.5.

4.1 Importance of transport processes on the time of the O_3 maxima

Tropospheric chemistry is controlled by multiple factors like concentrations of reactants or weather conditions (i.e. temperature). These weather conditions differ significantly across the troposphere. Our results show that air parcels with an early

https://doi.org/10.5194/acp-2020-46
Preprint. Discussion started: 31 January 2020

Atmospheric Chemistry and Physics Discussions

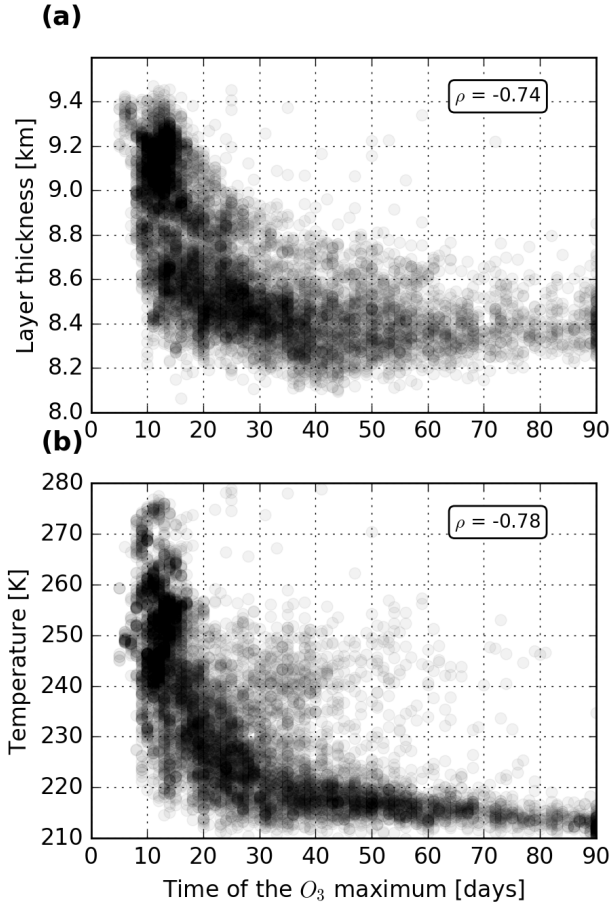

Figure 4. (a) Mean thickness of the 850 - 250 hPa layer. (b) Mean dry air temperature. Both are given in relation to the time when the O_3 maximum is reached. The mean value is based on the time span from emission until the maximum is reached. Data are taken from WP1. The Spearman rank correlation coefficient ρ is provided as a statistical measure.

maximum are characterised by a strong downward wind component, whereas late maxima have a weak downward or even an upward vertical wind component (not shown). Therefore, air parcels with an early O_3 maximum are transported to lower altitudes (Figure 3a) and lower latitudes (Figure 3b). Air parcels with a late maximum mostly stay at the emission altitude and latitude or are transported to higher altitudes and latitudes. For all winter patterns most maxima occur in a region spanning from 15°N to 35°N at pressure altitudes between 900 to 600 hPa. The maximum region is slightly shifted to higher altitudes for all summer patterns, which can be related to generally earlier maxima in summer, leaving less time for downward transport. No maximum occurs at high latitudes during winter due to the absence of solar radiation in the polar region during this time period. In total, this indicates that an early O_3 maximum only occurs if an air parcel is transported to lower altitudes and latitudes.

https://doi.org/10.5194/acp-2020-46
Preprint. Discussion started: 31 January 2020


Atmospheric Chemistry and Physics Discussions

Tropospheric vertical transport processes have many causes, e.g. temperature differences, incoming solar radiation, as well as latent and sensible heat. Vertical transport occurs in deep convection and conveyor belt events and causes an exchange of trace gases between the upper and the lower troposphere. Figure 4a shows the mean layer thickness of the 850 to 250 hPa layer. The layer thickness is proportional to the mean virtual temperature of the layer: a higher layer thickness indicates a higher temperature and moisture content. Air parcels with an early maximum have a higher mean layer thickness, whereas late maxima are associated with low layer thicknesses. In classical weather analysis, the layer thickness is used to identify synoptic weather systems. This indicates that in our study early maxima only occur if an air parcel originates or is transported into and stays within a high pressure system. No correlation exists between the time of the maximum and the layer thickness at emission (Spearman rank coefficient of -0.2). Still, air parcels originating within in the core of a high pressure system have generally earlier maxima compared to air parcel which are transported into high pressure systems after emission (not shown). It is well known that subsidence is dominating vertical transport processes within high pressure systems, explaining the strong downward motion of air parcels characterised by early maxima. Air parcels with late maxima stay within low pressure systems in which upward motion dominates.

Even though vertical transport is identified to be the main cause of earlier O_3 maxima, transport processes themself do not directly influence chemical processes in the atmosphere. Figure 4b shows the mean dry air temperature along the air parcel trajectory until the O_3 maximum is reached. The mean dry air temperature is higher for air parcels with early O_3 maxima, which is due to the downward and southward transport (leading to higher temperatures) within high pressure systems. Temperature is known to be a major factor controlling chemical processes in the atmosphere. These higher temperatures lead to higher background reaction rates and therefore accelerate foreground chemistry. The reaction rates for the production and loss of O_3 due to NO differ in their respective temperature dependency. Temperature has a low negative influence on the production rate coefficient but a strong positive impact on the destruction of O_3. Temperature generally decreases with increasing altitude (in the troposphere) and decreases towards higher latitudes. If an air parcel is transported to lower altitudes with higher temperatures, the chemical loss dominates the production of O_3 leading to a subsequent decrease of total O_3 and thus an earlier maximum. Higher temperatures during NH summer also explain the tendency of earlier maxima in this season.

4.2 Influence of background NO_x on total O_3 change in summer

A high mean air temperature causes an early maximum but only weakly correlates with the maximum O_3 concentration (Spearman rank coefficient about 0.5), suggesting that additional factors control the maximum O_3 gain. From classical chemistry, the production rate further depends on the reactants involved. In case of O_3 these are NO and HO_2 (Reaction R2). Figure 5 shows the dependency of the maximum O_3 concentration in relation to the mean NO_x concentration. Only low NO_x concentration will lead to high changes in O_3 concentrations. The production of O_3 via Reaction R2 to R4 dominates at low background NO_x concentrations, whereas at high background concentrations NO_2 is eliminated by reacting with OH and HO_2 forming nitric acid (HNO_3) and peroxynitric acid (HNO_4), respectively. In the upper troposphere the background NO_x concentration is altitude dependent and generally increases towards the tropopause (not shown). Air parcels with a fast downward transport, generally experience lower mean background NO_x concentrations resulting in a higher O_3 gain. Air parcels which stay close

https://doi.org/10.5194/acp-2020-46
Preprint. Discussion started: 31 January 2020

Atmospheric Chemistry and Physics Discussions

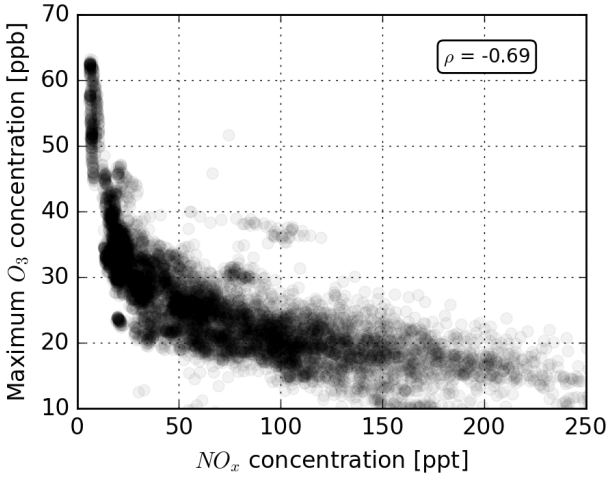

Figure 5. Maximum O_3 concentration in relation to the mean background NO_x concentration from emission until the maximum O_3 concentration is reached. Data are taken from SP3. The Spearman rank correlation coefficient ρ is provided as a statistical measure.

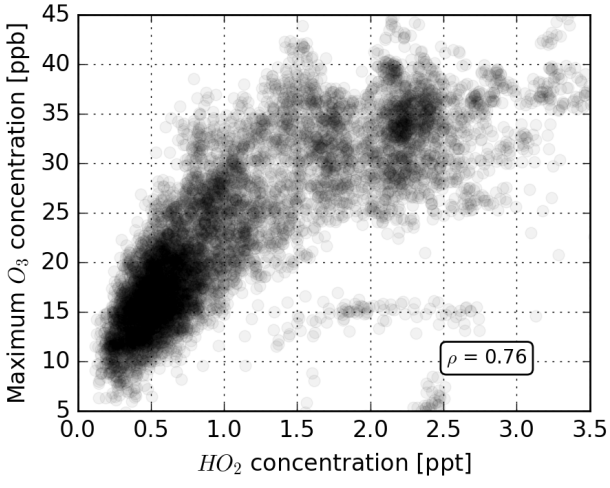

Figure 6. Maximum O_3 concentration in relation to the mean background HO_2 concentration from emission until the maximum O_3 concentration is reached. Data are taken from WP1. The Spearman rank correlation coefficient ρ is provided as a statistical measure.

to the tropopause or are even transported into the stratosphere experience a high background NO_x concentrations, leading to less O_3 being formed.

https://doi.org/10.5194/acp-2020-46
Preprint. Discussion started: 31 January 2020

Atmospheric Chemistry and Physics Discussions

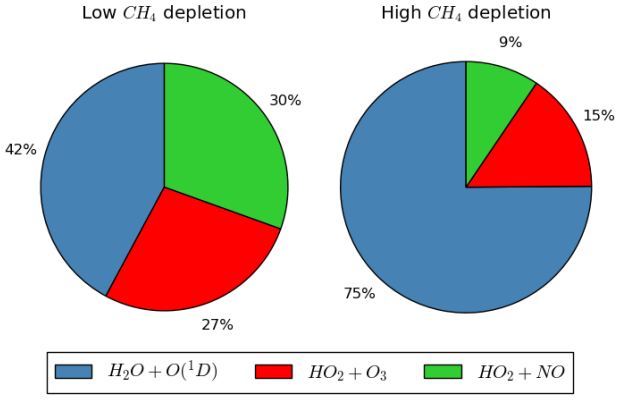

Figure 7. Relative contribution of all considered OH sources to the total background OH production. Air parcel with a total CH_4 depletion of more than 5 ppb are considered to have a high total CH_4 depletion. Results are valid for the first winter pattern.

4.3 Influence of background HO_2 on total O_3 change in winter

The background NO_x concentration strongly correlates with emissions in summer but weakly with emissions in winter. The Spearman rank coefficient for most winter pattern is below 0.44. During winter the maximum O_3 concentration correlates strongly with the mean background concentration of HO_2 (see Figure 6), the second reactant in Reaction R2. It becomes evident that only high background concentrations of HO_2 lead to a high formation of O_3. High background HO_2 concentrations dominate in high pressure systems (not shown). As for NO_x, HO_2 has a high variability throughout the troposphere and is generally lower in the upper troposphere and increases towards lower altitudes and latitudes. This explains why air parcels in high pressure systems experience higher HO_2 background concentrations, since they are quickly transported to lower altitudes and thus into areas where high HO_2 concentrations dominate.

The correlation of HO_2 and maximum O_3 during summer is rather weak (Spearman rank coefficient of about 0.40). Thus, it can be concluded that during summer the O_3 formation is limited by the background NO_x concentration, whereas in winter low HO_2 concentrations limit the total O_3 gained.

4.4 Influence of water vapour on the total CH_4 depletion

A high O_3 concentration may lead to a high CH_4 depletion (Spearman rank coefficient of 0.66) since O_3 is a major source of OH, accelerating the depletion of CH_4 (Reaction R5). However, the moderate Spearman rank coefficient indicates that other factors additionally control the CH_4 depletion process. Our results show that a high foreground CH_4 depletion is only possible if the background OH concentration is high. Air parcels with high CH_4 depletion experience a three times higher total OH production in the background compared to air parcels with low CH_4 depletion. In the modelling approach used, three sources of hydroxyl radicals were tagged: (1) the reaction of water vapour with exited oxygen atoms ($O(^1D)$), (2) the reaction of

https://doi.org/10.5194/acp-2020-46
Preprint. Discussion started: 31 January 2020

Atmospheric Chemistry and Physics Discussions

hydoperoxyl radicals (HO_2) with ozone and (3) with nitrogen oxide. Figure 7 shows the relative contribution of each major source to the background OH production for low and high CH_4 depletion. Here, air parcel with a total CH_4 depletion of more than 5 ppb are considered to have a high total CH_4 depletion. It becomes evident that the contribution to background OH differs significantly and almost twice as much OH is produced due to the reaction involving water vapour for the high CH_4 depletion case. Globally, Lelieveld et al. (2016) estimate that about 30% of the tropospheric OH is produced by this reaction, taking additional sources into account. This suggests that air parcels experiencing high CH_4 depletion are on average exposed to a higher water vapour content than the average troposphere. The highest CH_4 depletion rate occurs in tropical regions close to the surface (between 0°and 20°N and below 850hPa), which is dominated by hot and humid weather conditions. This region is known to have high HO_x (=OH+HO_2) concentrations due to active photochemistry and large OH sources and sinks. Here, the contribution of OH being produced by water vapour is highest (Lelieveld et al., 2016). The importance of water vapour is further strengthened by a strong correlation between the average specific humidity along the air parcel trajectory and the total depletion of CH_4 (Spearman rank coefficient above 0.71).

While O_3 is gained most foreground OH is produced by HO_2 reacting with NO (see Figure 1). In this period 35% and 42% of background OH is produced by HO_2 reacting with O_3 and NO, respectively. Due to the higher air parcel altitude during the O_3 gain, H_2O is only a minor source of OH.

The importance of O_3 as an OH source increases with increasing foreground O_3 concentration. In Figure 1, this can be clearly seen by an increasing CH_4 depletion rate between day five and ten. The larger background CH_4 depletion due to higher OH concentrations at lower altitudes explains why air parcels with an early O_3 maximum due to a strong downward transport and a high total O_3 gain experience a larger total CH_4 depletion. Therefore, a larger cooling effect due to a larger depletion of CH_4 is only possible for air parcels with a high O_3 formation by NO_x and if those air parcels are then transported into regions which are dominated by a high water vapour content. The transport into tropical regions, which are characterised by those conditions, occurs mainly due to the subsidence in high pressure systems (see Section 4.1).

4.5 Inter seasonal variability

Within this study specific weather situations (for graphical representations see Irvine et al. (2013, Figure 7 and Figure 8), and Frömming et al. (2020)) were analysed. Table 1 shows an overview of all correlations analysed within this study for each distinct weather pattern. Vertical transport processes, represented by the vertical wind velocity correlate reasonably well within both seasons. However, during summer the correlation tends to be lower. Summer pattern 3 has the lowest correlation coefficient and the highest mean downward wind velocity. The pattern is characterised by a high pressure blocking situation, resulting in an overall high layer thickness. This weakens the distinction between high and low pressure systems which explains the weaker correlation. Thus it is expected that differences in each individual weather situation (i.e. number, location and strength of the high pressure systems) cause the inter-seasonal variability. Additionally downward transport during summer is less important for air parcels to experience high temperatures. This also explains the weaker correlation for the 850 to 250 hPa layer thickness during summer. Still, air parcels which stay in a high pressure region experience earlier maxima during summer.

https://doi.org/10.5194/acp-2020-46
Preprint. Discussion started: 31 January 2020

Atmospheric Chemistry and Physics Discussions

Table 1. Spearman rank coefficient for all relations identify within in this study given for each individual weather pattern taken into account.

Correlation factors		Winter				Summer		
		WP1	WP3	WP4	WP5	SP1	SP2	SP3
Time of O_3 maximum	Vertical wind velocity	-0.67	-0.77	-0.69	-0.61	-0.66	-0.66	-0.57
	850 -250 hPa layer thickness	-0.74	-0.66	-0.61	-0.63	-0.59	-0.63	-0.56
	Mean temperature	-0.78	-0.84	-0.80	-0.79	-0.86	-0.82	-0.81
Maximum O_3	Mean background NO_x	-0.08	-0.37	-0.43	-0.66	-0.73	-0.76	-0.78
	Mean background HO_2	0.76	0.71	0.71	0.38	0.38	0.21	0.40
Total CH_4 depletion	Specific humidity	0.81	0.82	0.82	0.75	0.74	0.71	0.72

The mean background concentration of NO_x correlates strongly with the O_3 magnitude for each summer pattern, giving no indication that there is another parameter that controls the total O_3 gain. However, no correlation exists for most winter patterns. Only winter pattern five shows a strong correlation. When visually inspecting (not shown) the given correlation, it becomes evident that it looks almost the same as for SP3 (Figure 5) with the main difference that the maximum background NO_x concentration is lower but still significantly higher than for the other winter pattern. Winter pattern five also correlates weakly with the mean background HO_2 concentration. This indicates that the maximum O_3 concentration is limited by a combination of HO_2 and NO_x. The chosen example of winter pattern five occurs at the end February, whereas the other winter patterns are initialised in December or early January. This indicates that the controlling influence of HO_2 changes towards spring. This suggests that our results are only valid for the both analysed seasons and further research is necessary to identify the controlling factors in spring and autumn.

Specific humidity is clearly the controlling factor of the total CH_4 depletion for all weather patterns taken into account. Again the correlation is weaker for summer which can be explained by generally higher H_2O concentrations. This results in a lower variability in the specific humidity which weakens the correlation analysed. Here, winter pattern five again behaves like all summer patterns. This indicates that O_3 and CH_4 concentration changes due to emissions in spring are most likely controlled by mechanisms identified for summer.

5 Uncertainties and discussion

Our results indicate a large impact of transport patterns on ozone and methane concentration changes resulting from aviation NO_x emissions. This is both a highly complex interaction of transport and chemistry and relatively small contribution of ozone and methane concentration changes against a large natural variability. Hence a direct validation of our results is not feasible. However, the main processes, such as transport and chemistry can be evaluated individually - at least in parts. Hence we will discuss in the following some aspects of this interaction and discuss the ability of EMAC to reproduce observations.

https://doi.org/10.5194/acp-2020-46
Preprint. Discussion started: 31 January 2020


Atmospheric Chemistry and Physics Discussions

An important aspect in our study is the model's transport. Short-lived species which only have a surface source, such as ^{222}Radon (^{222}Rn, radioactive decay half-lifetime of 3.8 d), are frequently used to validate fast vertical transport characteristics. Jöckel et al. (2010) and in more detail Brinkop and Jöckel (2019) showed that the model is able to capture the ^{222}Rn surface concentrations and vertical profiles, indicating that the vertical transport is well represented in EMAC.

The horizontal transport is difficult to evaluate and observed trace gases, which resemble the exchange between mid and high latitudes and the tropics, are not available. However, Orbe et al. (2018) compared transport timescales in various global models, e.g. from northern mid-latitudes to tropics, which differed by 30% or interhemispheric transport, which differed by 20%. The authors concluded that vertical transport is a major source of this variability. More research is needed to better constrain models with respect to their tropospheric transport timescales. A more integrated view on the variability of aviation related transport-chemistry interaction is given by a model intercomparison of NO_x concentration differences between a simulation with and without aircraft NO_x emissions (Søvde et al., 2014, see their supplementary material). Here, we concentrate on the winter results to reduce the chemical impact to a minimum. The results clearly show a very similar NO_x change of the 5 models peaking around 40°N at cruise altitude in winter with a tendency to have a downward and southward transport to the tropics. However, the peak values vary between 55 pptv and 70 pptv.

Chemistry, or more specific, the concentrations of chemically active species is evaluated in detail in Jöckel et al. (2010) and Jöckel et al. (2016). In general EMAC overestimates the concentrations of tropospheric ozone by 5-10 DU in mid-latitudes and 10-15 DU in the tropics. Carbon monoxide on the other hand is underestimated, though the variability matches well with observations. The tropospheric oxidation capacity is at the lower end of model's estimates, but within the models' uncertainty ranges. Jöckel et al. (2016) speculate that lightning NO_x emissions or stratosphere-to-troposphere exchange might play a role. It is important to note that variations, which are caused by meteorology are in most cases well represented (e.g. Grewe et al., 2017a, their sec. 3.2).

Ehhalt and Rohrer (1995) already stated that the net-O_3 gain strongly depends in a non-linear manner on the NO_x mixing ratio. This is generally well reproduced in EMAC (Mertens et al., 2018, Figure 5) and even by an EMAC predecessor model (Dahlmann et al., 2011; Grewe et al., 2012, their Figure 4 and Figure 1, respectively). Stevenson et al. (2004) showed the response of ozone and methane to a pulse NO_x emission, which is very similar to our results (Grewe et al., 2014, their Figure 9). Stevenson and Derwent (2009) demonstrated that the NO_x concentration at time of emissions strongly defines the resulting climate impact of O_3. A similar but weaker relation can be found in the current data set (not shown) (Grewe et al., 2014, their Figure 9). For some air parcels the background NO_x concentration is low at time of emission but they are quickly transported to areas with higher concentrations. Thus, they experience a temporal high O_3 gain but only little total O_3 is formed, explaining the difference between our correlation and the one of Stevenson and Derwent (2009). Therefore, it can be concluded that not only the atmospheric conditions at emission influences the O_3 gain but rather the region in which the maximum O_3 concentration and the maximum concentration change occur. The findings of Stevenson and Derwent (2009) are also only valid for summer and no winter analysis is provided, making it impossible to compare our findings identified in Section 4.3.

https://doi.org/10.5194/acp-2020-46
Preprint. Discussion started: 31 January 2020


Atmospheric Chemistry and Physics Discussions

To conclude, both transport and chemistry processes are crucial for our results. EMAC is in many aspects in line with other model results, but has some biases in the concentration of chemical species. However, the variability of chemical species, such as NO_x and O_3 is better represented than mean values, indicating that the interaction between transport and chemistry is reasonably well simulated. Since our results show a very strong relation between meteorology and the contribution of aviation emission and since this interaction is in principle well represented in EMAC, this result should be robust. However, the strength of, e.g. the ozone response to a NO_x emission in a high pressure system has an uncertainty, which we hardly can estimate. Based on on the results of the model intercomparison by Søvde et al. (2014), we would expect an uncertainty in the order of 25%.

6 Conclusions

The possibility to reduce aviation's climate impact by avoiding climate sensitive regions, heavily depends on our understanding of the driving influences on induced contributions to the chemical composition of the atmosphere. In this study we demonstrated the importance of transport processes on locally induced aviation attributed NO_x emission on ozone and methane concentrations over the North Atlantic flight sector.

The resulting climate impact due to changes in ozone concentrations depends on the maximum ozone gained, where only early maxima result in a large ozone concentration change. Transport processes like subsidence in high pressure systems lead to early maxima, due to the fast transport into warmer regions. In summer the NO_x-HO_x-relation is limited by background NO_x, whereas in winter the limiting factor are the HO_2 concentrations. High NO_x concentrations in summer lead to lower changes in total ozone, since less ozone is formed in the background. In this case most NO_2 is eliminated by forming nitric acid and peroxynitric acid. During winter background HO_2 limits the total ozone gain, due to generally lower NO_x concentrations in the area of interest. Air parcels transported quickly towards lower altitudes encounter higher HO_2 concentrations leading to a higher ozone formation.

The total depletion of methane depends heavily on the background OH concentration. Since the major tropospheric source of OH is water vapour, the water vapour content the air parcel experiences along its trajectory defines the total methane depletion. Air parcels transported into lower altitudes and latitudes experience higher water vapour concentrations. Thus, atmospheric transport processes also define the total methane depletion. Additionally, only a high total gain of ozone allows a large methane depletion.

Due to the complexity of the problem, we are not able to validate our results. It would be challenging to design a measurement campaign to proof the contribution of aviation NO_x emissions to ozone and methane. The standard deviation of background concentrations are generally considered to be higher than changes induced by aviation NO_x perturbation, making them hardly detectable (Wauben et al., 1997). Our analysis of the model performance however shows that both transport processes as well as chemical concentrations are reasonably well represented. Our inter seasonal analysis shows that our findings to the importance of background NO_x and HO_2 concentrations are only valid for both seasons analysed. During summer background NO_x concentrations limit the total ozone gained. We expect other important factors to control the total ozone gain in other

https://doi.org/10.5194/acp-2020-46
Preprint. Discussion started: 31 January 2020


Atmospheric Chemistry and Physics Discussions

regions not analysed in this study, due to the high variability of NO_x concentrations in the troposphere. Based on the findings of Köhler et al. (2013), we expect our results to be valid for most part of the northern extra-tropics. To conclude, further model studies are necessary to fully quantify how transport processes influence induced changes of ozone and methane concentrations in all seasons as well as other regions of interest.

Calculating the climate cost for the re-routing of flight trajectories on a day to day basis is computationally too expensive to be feasible at the moment, if the same time horizon of 90 days was used as in REACT4C for simulating aircraft NO_x effects. Our results show that transport processes are of most interest when identifying the impact of local NO_x emissions on ozone and methane. Since, purely dynamic simulations without chemistry are less computationally expensive, the insights gained in this work can be used to allow a more feasible approach by only looking at transport processes. Our results show that concentration changes of ozone on methane induced by aviation NO_x mainly occur within the first twenty days. Therefore, an alternative approach could be to use shorter simulations to estimate the induced concentration changes and thus reduce computation costs significantly.

Data availability. The data of the REACT4C project used in this work are available on the REACT4C project home page (https://www.react4c.eu/, last access: 15 January 2020)

Author contributions. SR and VG designed the analysis and SR carried them out. CF performed the simulations of REACT4C. SR prepared the manuscript with contributions from all co-authors.

Competing interests. The authors declare that they have no conflict of interest.

Acknowledgements. This work was supported by the European Union FP7 Project REACT4C (Reducing Emissions from Aviation by Changing Trajectories for the benefit of Climate: www.react4c.eu/, Grant Agreement Number 233772) and contributes to the DLR project Eco2Fly. Computational resources were made available by the German Climate Computing Center (DKRZ) through support from the German Federal Ministry of Education and Research (BMBF) and by the Leibniz-Rechenzentrum (LRZ). We would like to thank Mariano Mertens from DLR for providing an internal review.

https://doi.org/10.5194/acp-2020-46
Preprint. Discussion started: 31 January 2020

Atmospheric Chemistry and Physics Discussions

References

Brasseur, G., Cox, R., Hauglustaine, D., Isaksen, I., Lelieveld, J., Lister, D., Sausen, R., Schumann, U., Wahner, A., and Wiesen, P.: European scientific assessment of the atmospheric effects of aircraft emissions, Atmospheric Environment, 32, 2329 – 2418, https://doi.org/https://doi.org/10.1016/S1352-2310(97)00486-X, 1998.

Brasseur, G. P., Gupta, M., Anderson, B. E., Balasubramanian, S., Barrett, S., Duda, D., Fleming, G., Forster, P. M., Fuglestvedt, J., Gettelman, A., Halthore, R. N., Jacob, S. D., Jacobson, M. Z., Khodayari, A., Liou, K.-N., Lund, M. T., Miake-Lye, R. C., Minnis, P., Olsen, S., Penner, J. E., Prinn, R., Schumann, U., Selkirk, H. B., Sokolov, A., Unger, N., Wolfe, P., Wong, H.-W., Wuebbles, D. W., Yi, B., Yang, P., and Zhou, C.: Impact of Aviation on Climate: FAA's Aviation Climate Change Research Initiative (ACCRI) Phase II, Bulletin of the American Meteorological Society, 97, 561–583, https://doi.org/10.1175/BAMS-D-13-00089.1, 2016.

Brinkop, S. and Jöckel, P.: ATTILA 4.0: Lagrangian advective and convective transport of passive tracers within the ECHAM5/MESSy (2.53.0) chemistry–climate model, Geoscientific Model Development, 12, 1991–2008, https://doi.org/10.5194/gmd-12-1991-2019, 2019.

Dahlmann, K., Grewe, V., Ponater, M., and Matthes, S.: Quantifying the contributions of individual NO_x sources to the trend in ozone radiative forcing, Atmospheric Environment, 45, 2860 – 2868, https://doi.org/https://doi.org/10.1016/j.atmosenv.2011.02.071, 2011.

Ehhalt, D. and Rohrer, F.: The impact of commercial aircraft on tropospheric ozone, Special Publication-Royal Society of Chemistry, 170, 105–120, 1995.

Frömming, C., Grewe, V., Brinkop, S., and Jöckel, P.: Documentation of the EMAC submodels AIRTRAC 1.0 and CONTRAIL 1.0, supplement of Grewe et al. (2014), 2013.

Frömming, C., Ponater, M., Dahlmann, K., Grewe, V., Lee, D. S., and Sausen, R.: Aviation-induced radiative forcing and surface temperature change in dependency of the emission altitude, Journal of Geophysical Research: Atmospheres, 117, https://doi.org/10.1029/2012JD018204, 2012.

Frömming, C., Grewe, V., Brinkop, S., Haslerud, A. S., Rosanka, S., van Manen, J., and Matthes, S.: Influence of the actual weather situation on aviation climate effects: The REACT4C Climate Change Functions (in preparation for Atmospheric Chemistry and Physics), 2020.

Gilmore, C. K., Barrett, S. R. H., Koo, J., and Wang, Q.: Temporal and spatial variability in the aviation NO_x-related O_3 impact, Environmental Research Letters, 8, 034 027, https://doi.org/10.1088/1748-9326/8/3/034027, 2013.

Grewe, V., Tsati, E., and Hoor, P.: On the attribution of contributions of atmospheric trace gases to emissions in atmospheric model applications, Geoscientific Model Development, 3, 487–499, https://doi.org/10.5194/gmd-3-487-2010, 2010.

Grewe, V., Dahlmann, K., Matthes, S., and Steinbrecht, W.: Attributing ozone to NO_x emissions: Implications for climate mitigation measures, Atmospheric Environment, 59, 102 – 107, https://doi.org/https://doi.org/10.1016/j.atmosenv.2012.05.002, 2012.

Grewe, V., Frömming, C., Matthes, S., Brinkop, S., Ponater, M., Dietmüller, S., Jöckel, P., Garny, H., Tsati, E., Dahlmann, K., Søvde, O. A., Fuglestvedt, J., Berntsen, T. K., Shine, K. P., Irvine, E. A., Champougny, T., and Hullah, P.: Aircraft routing with minimal climate impact: the REACT4C climate cost function modelling approach (V1.0), Geoscientific Model Development, 7, 175–201, https://doi.org/10.5194/gmd-7-175-2014, 2014.

Grewe, V., Dahlmann, K., Flink, J., Frömming, C., Ghosh, R., Gierens, K., Heller, R., Hendricks, J., Jöckel, P., Kaufmann, S., Kölker, K., Linke, F., Luchkova, T., Lührs, B., Van Manen, J., Matthes, S., Minikin, A., Niklaß, M., Plohr, M., Righi, M., Rosanka, S., Schmitt, A., Schumann, U., Terekhov, I., Unterstrasser, S., Vázquez-Navarro, M., Voigt, C., Wicke, K., Yamashita, H., Zahn, A.,

https://doi.org/10.5194/acp-2020-46
Preprint. Discussion started: 31 January 2020

Atmospheric Chemistry and Physics Discussions

and Ziereis, H.: Mitigating the Climate Impact from Aviation: Achievements and Results of the DLR WeCare Project, Aerospace, 4, https://doi.org/10.3390/aerospace4030034, 2017a.

Grewe, V., Matthes, S., Frömming, C., Brinkop, S., Jöckel, P., Gierens, K., Champougny, T., Fuglestvedt, J., Haslerud, A., Irvine, E., and Shine, K.: Feasibility of climate-optimized air traffic routing for trans-Atlantic flights, Environmental Research Letters, 12, 034 003, https://doi.org/10.1088/1748-9326/aa5ba0, 2017b.

Grewe, V., Tsati, E., Mertens, M., Frömming, C., and Jöckel, P.: Contribution of emissions to concentrations: the TAGGING 1.0 submodel based on the Modular Earth Submodel System (MESSy 2.52), Geoscientific Model Development, 10, 2615–2633, https://doi.org/10.5194/gmd-10-2615-2017, 2017c.

Irvine, E. A., Hoskins, B. J., Shine, K. P., Lunnon, R. W., and Froemming, C.: Characterizing North Atlantic weather patterns for climate-optimal aircraft routing, Meteorological Applications, 20, 80–93, https://doi.org/10.1002/met.1291, 2013.

Jöckel, P., Kerkweg, A., Pozzer, A., Sander, R., Tost, H., Riede, H., Baumgaertner, A., Gromov, S., and Kern, B.: Development cycle 2 of the Modular Earth Submodel System (MESSy2), Geoscientific Model Development, 3, 717–752, https://doi.org/10.5194/gmd-3-717-2010, 2010.

Jöckel, P., Tost, H., Pozzer, A., Kunze, M., Kirner, O., Brenninkmeijer, C. A. M., Brinkop, S., Cai, D. S., Dyroff, C., Eckstein, J., Frank, F., Garny, H., Gottschaldt, K.-D., Graf, P., Grewe, V., Kerkweg, A., Kern, B., Matthes, S., Mertens, M., Meul, S., Neumaier, M., Nützel, M., Oberländer-Hayn, S., Ruhnke, R., Runde, T., Sander, R., Scharffe, D., and Zahn, A.: Earth System Chemistry integrated Modelling (ESCiMo) with the Modular Earth Submodel System (MESSy) version 2.51, Geoscientific Model Development, 9, 1153–1200, https://doi.org/10.5194/gmd-9-1153-2016, 2016.

Kärcher, B.: Formation and radiative forcing of contrail cirrus, Nature Communications, 9, 1824, https://doi.org/10.1038/s41467-018-04068-0, 2018.

Köhler, M., Rädel, G., Shine, K., Rogers, H., and Pyle, J.: Latitudinal variation of the effect of aviation NO_x emissions on atmospheric ozone and methane and related climate metrics, Atmospheric Environment, 64, 1 – 9, https://doi.org/https://doi.org/10.1016/j.atmosenv.2012.09.013, 2013.

Köhler, M. O., Rädel, G., Dessens, O., Shine, K. P., Rogers, H. L., Wild, O., and Pyle, J. A.: Impact of perturbations to nitrogen oxide emissions from global aviation, Journal of Geophysical Research: Atmospheres, 113, https://doi.org/10.1029/2007JD009140, 2008.

Lacis, A. A., Wuebbles, D. J., and Logan, J. A.: Radiative forcing of climate by changes in the vertical distribution of ozone, Journal of Geophysical Research: Atmospheres, 95, 9971–9981, 1990.

Lee, D. S., Fahey, D. W., Forster, P. M., Newton, P. J., Wit, R. C., Lim, L. L., Owen, B., and Sausen, R.: Aviation and global climate change in the 21st century, Atmospheric Environment, 43, 3520 – 3537, https://doi.org/https://doi.org/10.1016/j.atmosenv.2009.04.024, 2009.

Lelieveld, J., Gromov, S., Pozzer, A., and Taraborrelli, D.: Global tropospheric hydroxyl distribution, budget and reactivity, Atmospheric Chemistry and Physics, 16, 12 477–12 493, https://doi.org/10.5194/acp-16-12477-2016, 2016.

Matthes, S.: Climate-optimised flight planning–REACT4C in Innovation for a Sustainable Avation in a Global Environment, Proceedings of the Sixth European Aeronautics Days, 2011.

Matthes, S., Schumann, U., Grewe, V., Frömming, C., Dahlmann, K., Koch, A., and Mannstein, H.: Climate Optimized Air Transport, pp. 727–746, Springer Berlin Heidelberg, Berlin, Heidelberg, https://doi.org/10.1007/978-3-642-30183-4_44, 2012.

Mertens, M., Grewe, V., Rieger, V. S., and Jöckel, P.: Revisiting the contribution of land transport and shipping emissions to tropospheric ozone, Atmospheric Chemistry and Physics, 18, 5567–5588, https://doi.org/10.5194/acp-18-5567-2018, 2018.

https://doi.org/10.5194/acp-2020-46
Preprint. Discussion started: 31 January 2020

Orbe, C., Yang, H., Waugh, D. W., Zeng, G., Morgenstern, O., Kinnison, D. E., Lamarque, J.-F., Tilmes, S., Plummer, D. A., Scinocca, J. F., Josse, B., Marecal, V., Jöckel, P., Oman, L. D., Strahan, S. E., Deushi, M., Tanaka, T. Y., Yoshida, K., Akiyoshi, H., Yamashita, Y., Stenke, A., Revell, L., Sukhodolov, T., Rozanov, E., Pitari, G., Visioni, D., Stone, K. A., Schofield, R., and Banerjee, A.: Large-scale tropospheric transport in the Chemistry–Climate Model Initiative (CCMI) simulations, Atmospheric Chemistry and Physics, 18, 7217–7235, https://doi.org/10.5194/acp-18-7217-2018, 2018.

Reithmeier, C. and Sausen, R.: ATTILA: atmospheric tracer transport in a Lagrangian model, Tellus B, 54, 278–299, https://doi.org/10.1034/j.1600-0889.2002.01236.x, 2002.

Roeckner, E., Bäuml, G., Bonaventura, L., Brokopf, R., Esch, M., Giorgetta, M., Hagemann, S., Kirchner, I., Kornblueh, L., Manzini, E., Rhodin, A., Schlese, U., Schulzweida, U., and Tompkins, A.: The atmospheric general circulation model ECHAM 5. Part I: Model description., Tech. Rep. 349, Max-Planck-Institute for Meteorology, Hamburg, 2003.

Sander, R., Kerkweg, A., Jöckel, P., and Lelieveld, J.: Technical note: The new comprehensive atmospheric chemistry module MECCA, Atmospheric Chemistry and Physics, 5, 445–450, https://doi.org/10.5194/acp-5-445-2005, 2005.

Shine, K. P., Derwent, R., Wuebbles, D., and Morcrette, J.: Radiative forcing of climate, in: Climate Change: The IPCC Scientific Assessment (1990), Report prepared for Intergovernmental Panel on Climate Change by Working Group I, edited by Houghton, J. T., Jenkins, G. J., and Ephraums, J. J., chap. 2, pp. 41–68, Cambridge University Press, Cambridge, Great Britain, New York, NY, USA and Melbourne, Australia, 1990.

Stevenson, D. S. and Derwent, R. G.: Does the location of aircraft nitrogen oxide emissions affect their climate impact?, Geophysical Research Letters, 36, https://doi.org/10.1029/2009GL039422, 2009.

Stevenson, D. S., Doherty, R. M., Sanderson, M. G., Collins, W. J., Johnson, C. E., and Derwent, R. G.: Radiative forcing from aircraft NO_x emissions: Mechanisms and seasonal dependence, Journal of Geophysical Research: Atmospheres, 109, https://doi.org/10.1029/2004JD004759, 2004.

Søvde, O. A., Matthes, S., Skowron, A., Iachetti, D., Lim, L., Owen, B., Øivind Hodnebrog, Genova, G. D., Pitari, G., Lee, D. S., Myhre, G., and Isaksen, I. S.: Aircraft emission mitigation by changing route altitude: A multi-model estimate of aircraft NO_x emission impact on O_3 photochemistry, Atmospheric Environment, 95, 468 – 479, https://doi.org/https://doi.org/10.1016/j.atmosenv.2014.06.049, 2014.

Wauben, W., Velthoven, P., and Kelder, H.: A 3D chemistry transport model study of changes in atmospheric ozone due to aircraft NO_x emissions, Atmospheric Environment, 31, 1819 – 1836, https://doi.org/https://doi.org/10.1016/S1352-2310(96)00332-9, 1997.

Wild, O., Prather, M. J., and Akimoto, H.: Indirect long-term global radiative cooling from NO_x Emissions, Geophysical Research Letters, 28, 1719–1722, https://doi.org/10.1029/2000GL012573, 2001.